Desalination and Water Treatment
www.deswater.com

doi:10.5004/dwt.2019.24074

153 (2019) 46–53
June

Development of heat and mass transfer coefficient correlations for natural packings used in solar desalination process

K. Zhani[a,b,*], S. Mejbri[b]

[a]*Department of Mechanical, College of Engineering, University of bisha, Bisha 61922, p.o.Box 199, Saudi Arabia, email: kzhani@ub.edu.sa (K. Zhani)*
[b]*LASEM (LAboratoire des Systemes Electro-Mecaniques), National Engineering School of Sfax, B.P. W3038, Sfax, Tunisia, email: mejbri_sami@yahoo.fr (S. Mejbri)*

Received 6 September 2018; Accepted 3 March 2019

ABSTRACT

Humidifiers are devices which increase the humidity of air or a carrier gas. They are used increasingly in a variety of applications such as heating, air conditioning, ventilation and desalination. The packing humidifier is the key component in solar desalination systems based on humidification and dehumidification principle. This paper focuses on developing a heat and mass transfer correlations for two types of natural packing, Thorn tree and palm leaves, used in solar desalination system. A mathematical model is developed for the packing humidifier based on heat and mass transfer balances. Several experimental tests were carried out on a test bench of an evaporation chamber, to determine the different heat and mass exchange coefficients at the contact surface of the two types of packing with the moist air. The effects of water and air mass flows are analyzed. It is shown that the heat and mass transfer coefficients increases with the increase of water and air mass flows. Correlations of mass and heat transfer coefficients are developed for each type of packing and compared with that given by the literature. Results show that the palm leaves are more efficient than the thorn trees. The developed correlations can be used to predict the packing size and the water and air outlet conditions of the packing humidifier.

Keywords: Solar desalination; Packed humidifier; Dynamic modeling; Simulation

1. Introduction

Humidifiers are used increasingly in a variety of applications such as heating, air conditioning, ventilation, water treatment, solar desalination and so on. In solar desalination systems with humidification and dehumidification process, the humidifier is the key component and it helps load the circulating air with high water vapour. Several different types of humidifier were used in solar desalination systems, such as tubular humidifiers [1], atomizing or spray humidifiers [2–4], wetted element or packed bed humidifiers [5–7], and bubble column humidifiers [8–11]. Due to uniform contact area all over the volume and great interface area, which allow a great value of heat and mass transfer rate consequently improves productivity and efficiency, packed humidifier seems most likely to be used in humidification and dehumidification solar desalination systems. A number of studies were conducted on solar packed humidification desalination with different types of packing material. Nematollahi et al. [12] presented an energy and energy analysis of solar packed bed humidification desalination with pall rings as packing material. It has been observed that the energy efficiency elevated with the reduction in the humidifier length. Amer et al. [13] investigated the humidifier efficiency of solar desalination system with different packing materials such as gunny bag cloth, plastic and wooden slates. It was found that High humidifier efficiency has been noticed with the wooden slates compared to the others. Muthusamy and Srithar [14] have used the gunny bag and saw dust as packing material in the humidifier of a HDH desalination. They concluded that the humidifier with gunny bag has better mass transfer coefficient and productivity compared to the saw dust as packing mate-

*Corresponding author.

rial. In addition to the above, textile material (viscose) [15]. Honey comb paper [16], wooden shavings [17], raschig ring ceramic [18], indigenous structure [19], wooden surface [20], canvas [21], a block of corrugated and treated cellulose paper [22] and plastic pad [23] have also been used as packing material in the humidification desalination process.

The main goals of this study are to propose two types of natural packing, Thorn tree and palm leaves, in order to resist to the problems caused by the nature of water used in solar desalination systems (high salinity level, chalky, solid residuals and corrosion problems, etc.) and to determine the heat and mass transfer correlations for the proposed natural packings.

2. Experimental apparatus and procedure

The experimental apparatus for the heat and mass transfer experiments consisted of a counter flow forced draft humidifier used in a new generation of water desalination unit by solar energy located at the national engineering school of S fax (34 N, 10 E), Tunisia, as shown in Fig. 1. Humidifiers are used in solar desalination systems to load water vapour into the air stream that passes in a counter flow direction such that air would be heated and humidified as shown in Fig. 2. The driving potential for heat transfer is temperature difference between both streams whereas another driving potential for mass transfer due to the difference in water-vapor concentration. Humidification rate is proportional to the contact surface of water and air streams. The artificial increase of this surface has been tried by packing's humidifier. Due to the nature of the water (hot salinity level, chalky, solid residuals and corrosion problems, etc.), the packing used in the humidifier must be carefully chosen. Thorn trees or palm tree leaves are well suited for this application. They are abundant, free and have a high resistance against the forth-mentioned problems. The structure of current packing's humidifier is made of aluminum profiles to resist the corrosive medium and support the multi directional stresses. From the outside and to ensure good thermal insulation, the walls and roof of this structure are formed by Styrofoam (extruded polystyrene foam) layers with a thickness of 40–50 mm. To insure leakage of circulating water vapor in the humidifier, and to protect the Styrofoam plates against corrosion caused by brackish water, the inside of the structure is covered by polypropylene sheets.

During the experiment, hot salt water coming from the water solar collector is sprayed over the packing such that the surface area would be large enough for interaction with air stream. The supply water velocity was regulated by a valve. The air fan located at the bottom of the humidifier draws ambient air to the latter at almost constant volumetric flow rate. The air flow rate is mea-

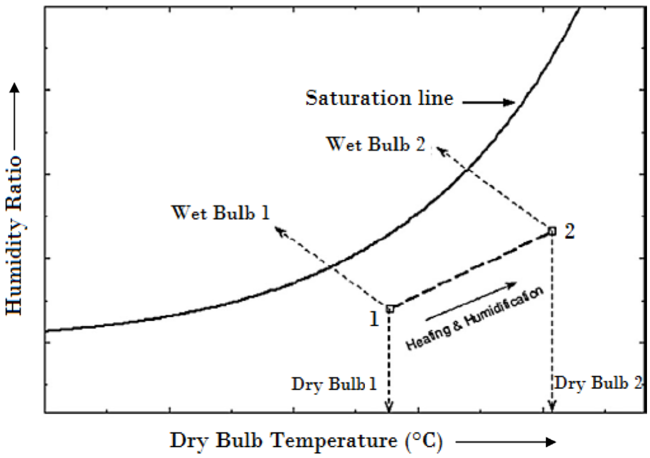

Fig. 2. Representation of the heating and humidification process on the psychrometric chart.

Fig. 1. A photo of the solar desalination unit experimental setup.

sured at the humidifier inlet using a digital anemometer. All temperatures are measured with Pt 100 thermistors with a sensibility of 0.3799X/°C. All the sensors, which were calibrated before using to determine the probes sensibility, were connected to a data acquisition system (type Agilent 34970A). During experimentation, all the parameters were measured and recorded every 1 min for up to 420 min.

3. Mathematical modelling of the packing

The method of setting up the mass, thermal and enthalpy balances will be undertaken with the following simplifying assumptions:

- The process is adiabatic,
- The air and water flows are in co-current and one-dimensional,
- The specific heat of water is constant during its passage by the humidifier,
- The equations are written as if the transfer were from water to air.

Consider a differential width, *dz*, across the contacting area as shown in Fig. 3, which shows the differential section of the contacting area is divided in three control volumes air, water and interface to set up the heat, mass and enthalpy balance equations.

- Thermal balance

–Air phase

The air thermal balance in the packing height volume element dz, is the following one:

$$GC_g dT_g = h_g a\left(T_i - T_g\right)dz \tag{1}$$

It can be further simplified as:

$$\frac{dT_g}{dz} = \frac{h_g a}{GC_g}\left(T_i - T_g\right) \tag{2}$$

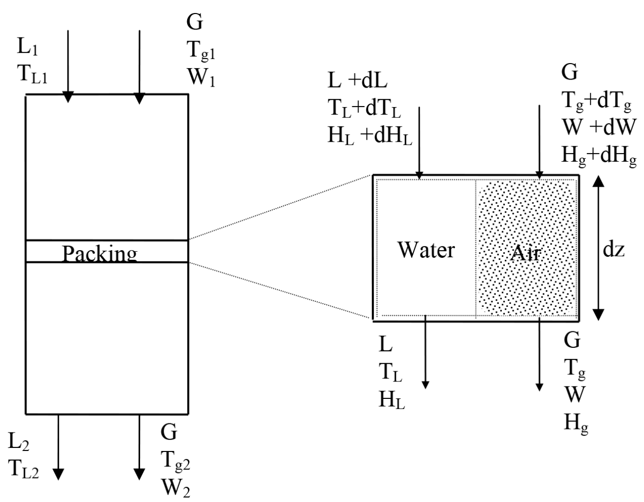

Fig. 3. Control volume of the packing.

–Water phase

The water thermal balance in the packing height volume element *dz*, is the following one:

$$h_L a\left(T_L - T_i\right)dz = LC_L dT_L \tag{3}$$

It can be further simplified as:

$$\frac{dT_L}{dz} = \frac{h_L a}{LC_L}\left(T_L - T_i\right) \tag{4}$$

- Enthalpy balance

The global equilibrium of the enthalpy is written as follows:

$$L_1 H_{L1} + GH_{g2} = L_2 H_{L2} + GH_{g1} \tag{5}$$

Or in a differential form,

$$d\left(LH_L\right) = GdH_g \tag{6}$$

– Enthalpy balance of air phase

The specific moist air enthalpy is :

$$H_g = C_g\left(T_g - T_o\right) + \lambda_o W_g \tag{7}$$

Given that the specific heat of moist air is, then the total differential change of the moist air enthalpy is defined as follows:

$$GdH_g = GC_g dT_g + GC_v T_g dW_g - GC_v T_o dW_g + G\lambda_o dW_g \tag{8}$$

$$GdH_g = GC_g dT_g + GC_v\left(T_g - T_o\right)dW_g + G\lambda_o dW_g \tag{9}$$

– Enthalpy balance of water phase

The total differential change in the water enthalpy is defined as follows:

$$d\left(LH_L\right) = LC_L dT_L + C_L\left(T_L - T_o\right)dL \tag{10}$$

$$d\left(LH_L\right) = GdH_g = GC_g dT_g + GC_v\left(T_g - T_o\right)dW_g + G\lambda_o dW_g \tag{11}$$

The combination of Eqns. (7) and (8) leads to the following equation:

$$\begin{aligned} &LC_L dT_L + C_L\left(T_L - T_o\right)dL = GC_g dT_g + \\ &GC_v\left(T_g - T_o\right)dW_g + G\lambda_o dW_g \end{aligned} \tag{12}$$

$$LC_L dT_L = G\left\{C_g dT_g + \left[C_v\left(T_g - T_o\right) - C_L\left(T_L - T_o\right) + \lambda_o\right]dW_g\right\} \tag{13}$$

or approximately,

$$LC_L dT_L \simeq GC_g dT_g + G\lambda_o dW_g \tag{14}$$

- Mass balance

$$K_m a\rho\left(W_i - W_g\right)dz = GdW_g \tag{15}$$

$$\frac{dW_g}{dz} = \frac{K_m a\rho}{G}\left(W_i - W_g\right) \tag{16}$$

The substitution of d_{Tg}, d_{Tl} and d_{Wg} by their respective Eqs. (1), (2) and (11) in Eq. (10) gives an equation that allows us to determine the water content at the interface. The analytical solution of the above ordinary differential equations is impossible and they must be discretized to obtain approximate, but still accurate, solutions. The fourth order Runge-Kutta method is used to solve the ordinary differential equations numerically.

4. Principle of the determination of heat and mass transfer correlations

The equations presented above make it possible to determine the temperatures and quantities of water and air at the humidifier outlet, depending on the input parameters. In order to be able to solve the obtained system of equations, it is necessary to know for given mass velocities of air and water, the coefficients of heat (h_l, h_g) and of mass (K_m) exchanges for the type of used packing. The coefficients of heat and mass exchanges of a packing are of a close connection with the temperature of the interface which is a priori unknown. To be able to solve the problem, one must minimize the number of variables to be determined. This is achieved by finding relationships between these coefficients. The air-film heat transfer coefficient and the mass transfer coefficient on the air–water interface are coupled by the Lewis relation [24] as follows:

$$h_g a = \alpha\rho C_g K_m a \tag{17}$$

$$\alpha = 4.275\ 10^{-4}\left(T_g - T_0\right) + 0.8726 \tag{18}$$

Using the above relationship, the number of variables has been reduced to two. In order to work with only one variable:

$$P = \frac{h_l a}{K_m a} \tag{19}$$

In the following, we will write all the previous equations as a function of P and α. Eqs. (15) and (13) give the following equation:

$$\frac{h_l a}{h_g a} = \frac{P}{\alpha\rho C_g} \tag{20}$$

By dividing Eq. (2) by Eq. (1), and writing it according to P we obtain

$$\frac{dT_l}{dT_g} = P\frac{\beta}{\alpha}\frac{\left(T_i - T_l\right)}{\left(T_g - T_i\right)} \tag{21}$$

With

$$\beta = \frac{G}{L\rho C_l} \tag{22}$$

Hence

$$T_i = \frac{P\beta T_l + \alpha T_g \dfrac{dT_l}{dT_g}}{\alpha\dfrac{dT_l}{dT_g} + P\beta} \tag{23}$$

By substituting Eqs. (15) and (16) in Eq. (12) we will have:

$$(W_i - W_g) = \frac{PT_l + \alpha\rho C_g T_g - (P + \alpha\rho C_g)T_i}{\rho\lambda_o} \tag{24}$$

By substituting Eq. (18) in Eq. (19) we will have:

$$W_i = W_g + \frac{P\alpha\dfrac{dT_l}{dT_g}\left(T_l - T_g\right) - \alpha\rho C_g P\beta\left(T_l - T_g\right)}{\left(\alpha\dfrac{dT_l}{dT_g} + P\beta\right)\lambda_O\rho} \tag{25}$$

Eqs. (18) and (20), as well as an additional equation, of the saturation curve of water vapor [24] will be used to determine P, W_i and T_i:

$$W_i = 0,62198\frac{P_{ws}}{1 - P_{ws}} \tag{26}$$

where P_{ws} is the partial saturation pressure of the water vapor corresponding to a certain temperature is computed from [25] as:

$$\ln\left(P_{ws}\right) = -6096.938\frac{1}{T_i} + 21.240964 - 2.7111910^{-2}T_i + 1.6739510^{-5}T_i^2 + 2.43350\ln\left(T_i\right) \tag{27}$$

5. Computational process

Fig. 4 shows the algorithm used to calculate the exchange coefficients. The height of the packing is subdivided into elements of infinitesimal volumes, d_V. The height d_z of each element d_V corresponds to the distance between two computation nodes. Each node will be characterized by water temperature, T_1, air temperature, T_g, interface temperature, T_i, air moisture content, W_g, and interface air moisture content, W_i. T_l, T_g, and W_g will be calculated from the polynomials $T_l(z)$, $T_g(z)$, and $W_g(z)$. The temperature of the interface in each node is a priori unknown. To determine it, we proceed as follows:

- Estimate T_i at (T_g+T_l) / 2, then calculate W_i using Eq. (20),
- Calculate $(K_m a)$ by the Eq. (23), obtained by solving Eq. (11)

$$K_m a = \frac{dW_g}{dz}\frac{G}{\rho\left(W_i - W_g\right)} \tag{28}$$

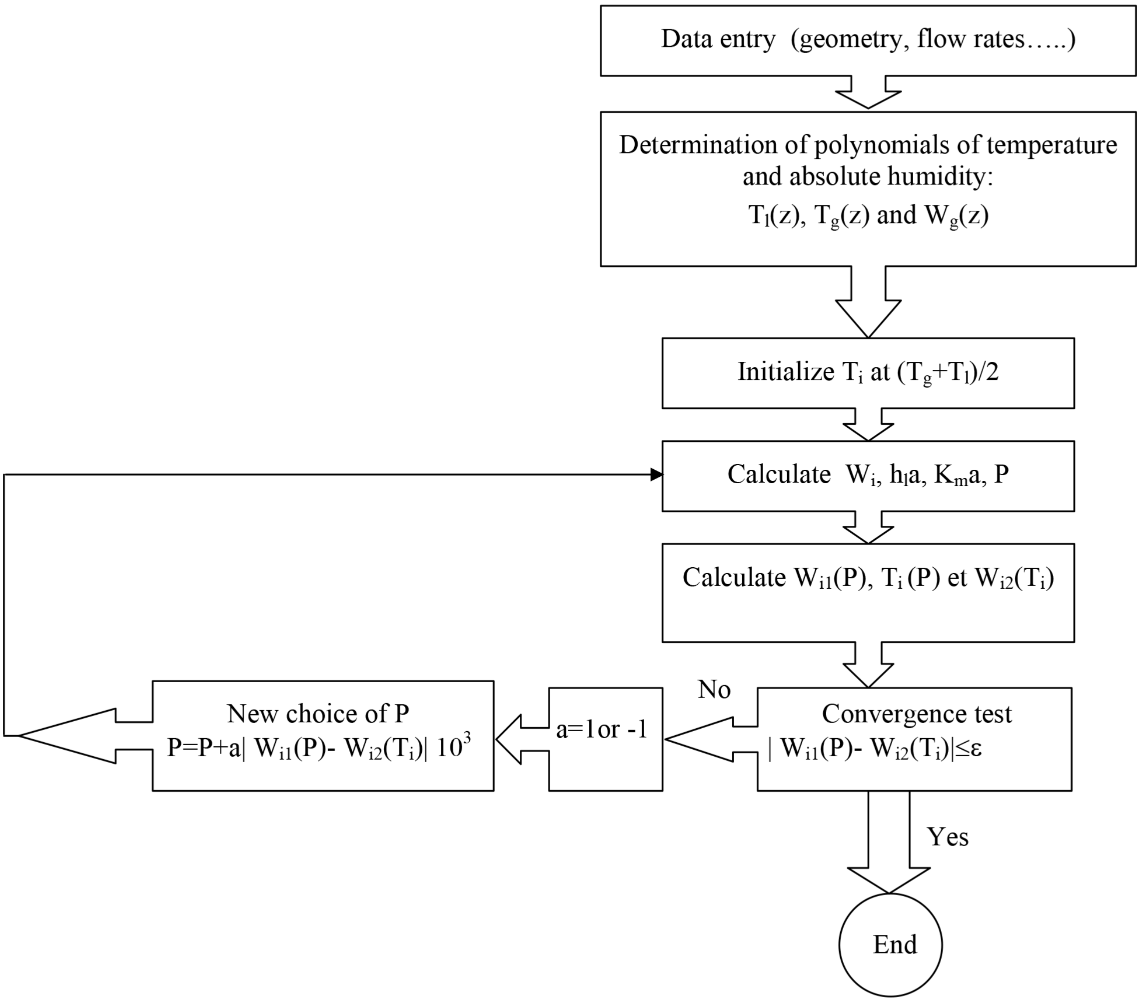

Fig. 4. The procedure (algorithm) used to calculate the exchange coefficients.

- Calculate $(h_l a)$ by the Eq. (24), obtained by solving Eq. (2)

$$h_l a = \frac{dT_l}{dz} \frac{\mathrm{L}C_l}{\left(T_l - T_i\right)} \tag{29}$$

then calculate P by Eq. (15),
- Calculate W_{i1} (P) by Eq. (21), T_i by Eq. (18), and W_{i2} (T_i) by Eq. (22),
- Compare W_{i1} and W_{i2} which must be equal for the good value of T_i. If we find a difference, we choose a new value of P to minimize the difference. The new value of P is given by the relation:

$$\mathrm{P} = \mathrm{P} + \mathrm{a}\left|W_{\mathrm{i1}} - \mathrm{W}_{\mathrm{i2}}\right|1000 \tag{30}$$

where a is a factor that takes the value of 1 or –1 whether if we want to increase or decrease *P*.

Using the value of *P*, one calculates T_i (P) by the Eq. (18), W_{i1} (P) by Eq. (20), W_{i2} (Ti) by Eq. (21) and the difference $(W_{i1} - W_{i2})$, then the new value P. This operation is repeated until $(W_{i1} - W_{i2})$ is lower than an error fixed in advance. Finally we determine $K_m a$ and $h_l a$ by Eqs. (23) and (24).

6. Results and discussion

Developing a correlation of the heat and mass transfer coefficients is necessary to predict the outlet conditions and packing height for the humidifier. Based on the values of mass and heat transfer coefficients calculated from experimental data, correlations are developed in this section. The determination of the values of the exchange coefficients consists in seeking a correlation between the exchange coefficients relative to each packing and the mass velocities of the air and the water. $K_m a = f(G, L)$, $h_l a = f(G, L)$, $h_g a = f(G, L)$. To find these correlations, series of tests are carried out on an experimental evaporation tower of 0.9 m² of section and 2 m of height. The tests consist in varying the flow of air and water. For each combination of flow rates, five equidistant levels of the height of the cooling tower are taken from the dry air temperature, the water temperature and the relative humidity. The moisture content of the moist air is then determined from the moist air diagram. Using the "Grapher" software, we make a polynomial smoothing of order 4 of the functions $T_l = f(z)$, $T_g = f(z)$ and $W_g = f(z)$. The values of *L, G*, the height of the tower and the coefficients of the three polynomials are introduced in the solving program of the system

Table 1
Comparisons of heat and mass transfer coefficients

Packing type	Mass transfer coefficient	Heat transfer coefficient	References
Palm leaves	$K_m a = 137.36\ G^{0.47}\ L^{0.94}$	$h_l a^*\ 36.07\ 10^4\ G^{0.9}\ L^{0.68}$	Present work
Thorn tree	$K_m a = 2.09\ G^{0.11515}\ L^{0.45}$	$h_l a\ ^*\ 5900\ G^{0.5894}\ L^{0.169}$	
Wood	$K_m a = 2.95\ G^{0.72}\ L^{0.26}$	$h_l a^*1.04\ .\ 104\ G\ L^{0.51}$	[26]
Cellulosic material	$K_m a^*\ 0.6119 G^{0.3753}\ L^{0.1002}\ Z^{-0.0986}$	$h_l a\ ^*\ 25223.5\ G^{0.1644}\ L^{0.0591}\ Z^{-0.0542}$	[27]
Woodenslats	$K_m aV/L = 0.52\ (L/G)^{-0.16}$	-	[28]
Woodenslats	$K_m aV/L = 1.19\ (L/G)^{-0.66}$	-	[29]
PVC	$K_m a = 1.20\ G^{0.6}\ L^{0.45}$	-	[30]

of equations, to have as output the values of h_g, h_1 and K_m. A careful review of the developed heat and mass transfer correlations showed in Table 1 indicates that these correlations are provided in the form of the power functions of L and G. For this reason if one of the two values of L and G is maintained constant, a logarithmic representation log *($h_l a$ or $K_m a$) = f (log (G or L))* results in obtaining the form: $h_l a$ or $K_m a = \alpha G\gamma\ L\eta$

Packing n° 1: Thorn tree

The branched bundles of thorn tree are stacked longitudinally in the packing column. The results of this packing test are shown in Figs. 5 and 6.

For values of G = 0.89 kg/m^2 s and L = 0.222 kg/m^{2}s, we find:

$$hl\ a = 5900\ G^{0,5894}\ L^{0,169} \quad (31)$$

$$K_m\ a = 2.09\ G^{0.11515}\ L^{0.45} \quad (32)$$

Packing n° 2: The palm leaves

The palm leaves are cut into pieces of 30 cm in length and are stacked crosswise with alternating orientations. The experimental tests, shown in Figs. 7 and 8, provided the following results:

For values of G = 0.827 kg/m^{2}s and L = 0.555 kg/m^{2}s, we find:

$$hl\ a = 36.07\ .\ 10^4\ G^{0,9}\ L^{0,68} \quad (33)$$

$$K_m a = 137.36\ G^{0.47}\ L^{0.94} \quad (34)$$

From the results depicted in Figs. 5–8, it can be seen that an increase in the water flow rate for a constant air flow rate or vice versa leads to an increase in the heat and mass exchange coefficients. This increases the amount of water evaporated and the thermal gradient between the inlet and the outlet parameters of the humidification process. For the same pair (water, air) of flow rates, the two tested types of packing, as well as that given by the literature review presented in Table 1, are differentiated by their exchange coefficients. It is clear that the palm leaves are more efficient than the thorn trees and the wood to garnish the humidification column. This seems obvious since the palm leaves offer a larger exchange surface per unit volume.

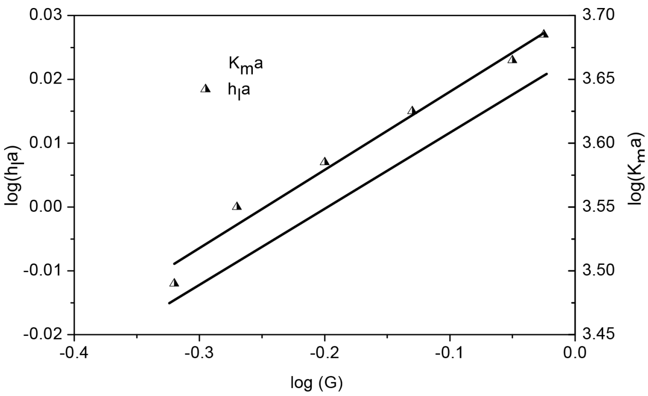

Fig. 5. Variations of heat and mass transfer coefficients of thorn tree as a function of water flow rate (L = 0.222 kg/m^{2}s).

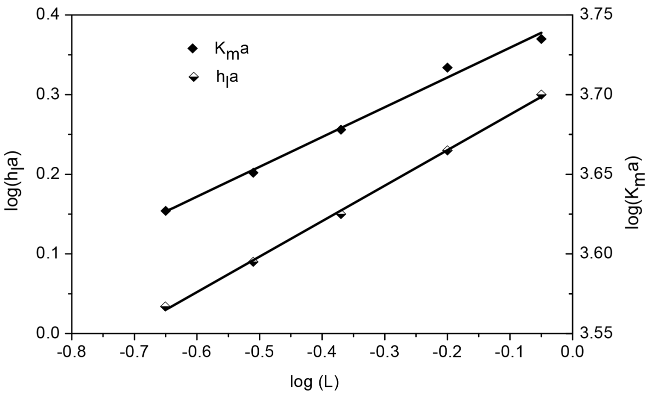

Fig. 6. Variations of heat and mass transfer coefficients of thorn tree as a function of airflow rate (G = 0.898 kg/m^{2}s).

7. Conclusion

Packed humidifiers are used increasingly in a variety of applications in the desalination systems. The reasons for this are an increase in the availability of design information, the evolution of higher-capacity for absorption and higher efficiency heat and mass transfer packings, and improvements in distributors and support plates. In this paper, Correlations of heat and mass transfer coefficients were developed for two types of natural packings,Thorn tree and palm leaves,and compared with that given by the literature.

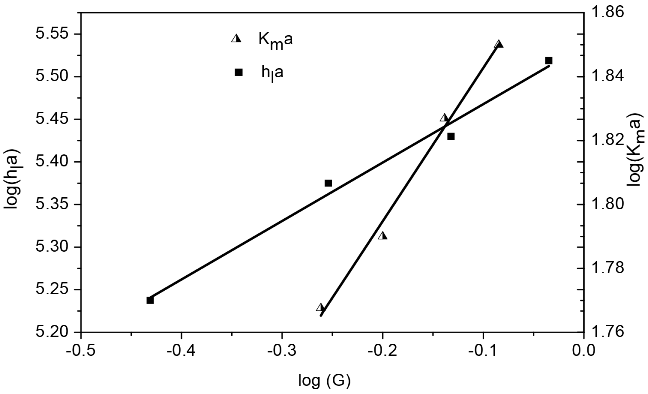

Fig. 7. Variations of heat and mass transfer coefficients of palm leaves as a function of air flow rate (L = 0.555 kg/m²s).

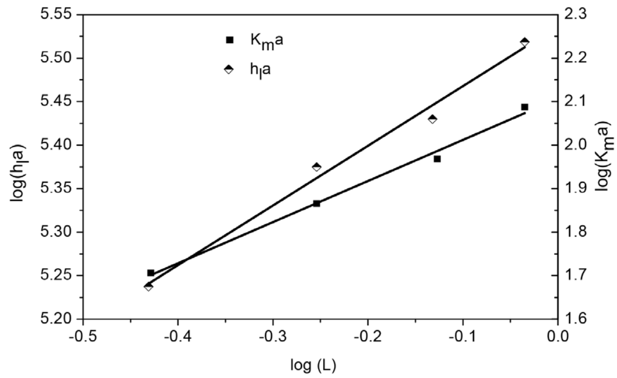

Fig. 8. Variations of heat and mass transfer coefficients of palm leaves as a function of water flow rate (G = 0.827 kg/m²s).

It was found that the palm leaves are more efficient than the thorn trees. It was also found that the heat and mass transfer coefficients increases with the increase of water and air mass flows. The developed correlations can be used to predict the packing size and the water and air outlet conditions of the packing humidifier.

Symbols

a	—	Specific mass transfer area (m²/m³)
C_g	—	Air specific heat (J/(kg·K))
C_l	—	Water specific heat (J/(kg·K))
C_v	—	Water vapor specific heat (J/(kg·K))
H	—	Enthalpy (kJ/kg)
G	—	Density of the mass flow of air (kg/(m²·s))
h	—	Heat transfer coefficient (J/(kg·K))
h_g	—	Air heat transfer coefficient at the air-water interface (W/(m²·K))
h_l	—	Water heat transfer coefficient at the air-water interface (W/(m²·K))
K_m	—	Water vapor mass transfer coefficient at the air-water interface (kg/(m²·s))
L	—	Density of the mass flow of water (kg/(m²·s))
P_{ws}	—	Saturation pressure (Pa)
T	—	Temperature(K)
T_o	—	Reference temperature conventionally at 0°C
V	—	Volume (m³)
W_g	—	Air humidity (kg water/kg dry air)
W_l	—	Saturation humidity (kg water/kg dry air)
L	—	Length of the humidifier packed bed (m)
z	—	Coordinate in the flow direction (m)

Greek

λ_o	—	Latent heat of water evaporation (J/kg)
α	—	Lewis coefficient
ρ	—	Density of moist air (kg/m³·s)

Subscripts

1	—	Inlet
2	—	Outlet
l	—	Water
g	—	Moist air

References

[1] S. Yanniotis, K. Xerodemas, Air humidification for sea water desalination, Desalination, 158 (2003) 313–319.
[2] I. Houcine, M.B. Amara, A. Guizani, M. Maâlej, Pilot plant testing of a new solar desalination process by a multiple-effect-humidification technique, Desalination, 196 (2006) 105–124.
[3] F. Kreith, R.F. Boehm Direct contact heat transfer, Washington: Hemisphere Corporation; 1988.
[4] M.B. Amara, I. Houcine, A. Guizani, M. Maalej, Experimental study of a multipl-effect humidification solar desalination technique, Desalination, 170 (2004) 209–221.
[5] M.I. Zubair , F.A. Al-Sulaiman, M.A. Antar, S.A. Al-Dini, N.I. Ibrahim, Performance and cost assessment of solar driven humidification dehumidification desalination system, Energy Convers. Manage., 132 (2017) 28–39.
[6] Y.J. Dai, H.F. Zhang, Experimental investigation of a solar desalination unit with humidification and dehumidification, Desalination, 130 (2000) 169–175.
[7] Y.J. Dai, R.Z. Wang, H.F. Zhang, Parametric analysis to improve the performance of a solar desalination unit with humidification and dehumidification, Desalination, 142 (2002) 107–118.
[8] K. Srithar, T. Rajaseenivasan, Performance analysis on a solar-bubble column humidification dehumidification desalination system, Process Saf. Environ., 105 (2017) 41–50.
[9] T. Rajaseenivasan, R.K. Shanmugam, V.M. Hareesh, K. Srithar, Combined probation of bubble column humidification dehumidification desalination system using solar collectors, Energy, 116 (2016) 459–469.
[10] H. Liu, M.H. Sharqawy, Experimental performance of bubble column humidifier and dehumidifier under varying pressure, Int. J. Heat Mass Transfer., 93 (2016) 934–944.
[11] S.A. El-Agouz, M. Abugderah, Experimental analysis of humidification process by air passing through seawater, Energy Convers Manage., 49 (2008) 3698–3703.
[12] F. Nematollahi, A. Rahimi, T.T. Gheinani Experimental and theoretical energy and exergy analysis for a solar desalination system, Desalination, 317 (2013) 23–31.
[13] E.H. Amer, H. Kotb, G.H. Mostafa, A.R. El-Ghalban, Theoretical and experimental investigation of humidification-dehumidification desalination unit, Desalination, 249 (2009) 949–959.

[14] C. Muthusamy, K. Srithar, Energy and energy analysis for a humidification–dehumidification desalination system integrated with multiple inserts, Desalination, 367 (2015) 49–59.
[15] K. Zhani, H.B. Bacha, Experimental investigation of a new solar desalination prototype using the humidification-dehumidification principle, Renew Energy, 35 (2010) 2610–2617.
[16] G. Yuan, HF. Zhang, Mathematical modeling of a closed circulation solar desalination unit with humidification-dehumidification, Desalination, 205 (2007) 156–162.
[17] M.M. Farid, A.W. Al-Hajaj, Solar desalination with humidification–dehumidification cycle, Desalination, 106 (1996) 427–429.
[18] A. Eslamimanesh, M.S. Hatamipour, Mathematical modeling of a direct contact humidification-dehumidification desalination process, Desalination, 237 (2009) 296–304.
[19] H.P. Garg, R.S. Adhikari, R. Kumar, Experimental design and computer simulation of multi-effect humidification (MEH) – dehumidification solar distillation, Desalination, 153 (2002) 81–86.
[20] S. Al-Hallaj, M.M. Farid, A.R. Tamimi, Solar desalination with humidification-dehumidification cycle: performance of the unit, Desalination, 120 (1998) 273–280.
[21] A.S. Nafey, H.E.S. Fath, S.O. El-Helaby, A.M. Soliman, Solar desalination using humidification-dehumidification processes. Part II. An experimental investigation, Energy Convers Manage., 45 (2004) 1263–1277.
[22] J.J. Hermosillo, C.A. Arancibia-Bulnes, C.A. Estrada, Water desalination by air humidification: mathematical model and experimental study, Sol. Energy, 86 (2011) 1070–1076.
[23] C. Yamali, I. Solmusf, A solar desalination system using humidification-dehumidification process: experimental study and comparison with the theoretical results, Desalination, 220 (2008) 538–551.
[24] ASHRAE, Fundamental handbook Tome V-1977.
[25] K. Zhani, H. Ben Bacha, Modeling simulation and experimental validation of a pad humidifier used in solar desalination process, Desal. Water Treat., 51(7–9) (2013) 1477–1486
[26] J.M. Coulson, J.F. Richardson, Chemical Engineering VI, 3rd ed., Pergamon Press, 1976.
[27] M.B. Amara, I. Houcine, A.A. Guizani, M. Mâalej, Theoretical and experimental study of a pad humidifier used on an operating seawater desalination process, Desalination, 168 (2004) 1–12.
[28] M.M. Farid, N.K. Nawayseh, S. Al-Hallaj, A.R. Tamimi, Solar desalination with humidification dehumidification process: studies of heat and mass transfer. In Proceeding of the Conference: Solar, 95 (1995) 293–306. Hobart, Tasmania.
[29] H.R. Goshayshi, J.F. Missenden, The investigation of cooling tower packing in various arrangements, Appl. Therm. Eng., 20 (2000) 69–80.
[30] N.K. Nawayseh, F.MM, A. A.-T., S. Al-hallaj, Solar desalination based on humidification process-I. Evaluating the heat and mass transfer coeffcients, Energy Convers. Manage., 40 (1999) 1423–1439.